UNITED STATES
DEPARTMENT OF THE INTERIOR
GEOLOGICAL SURVEY

GEODETIC TRISECTION, ALTITUDE, AND ICE-RADAR SURVEYING TECHNIQUES USED AT KNIK GLACIER, ALASKA, AND SUMMARY OF 1979, 1980, AND 1981 DATA

By L. R. Mayo and D. C. Trabant

U.S. GEOLOGICAL SURVEY

OPEN-FILE REPORT 82-685

Prepared in cooperation with the
ALASKA DEPARTMENT OF NATURAL RESOURCES,
DIVISION OF GEOLOGICAL AND GEOPHYSICAL SURVEYS

Fairbanks, Alaska
1982

UNITED STATES DEPARTMENT OF THE INTERIOR

JAMES G. WATT, Secretary

GEOLOGICAL SURVEY

Dallas L. Peck, Director

For additional information write to:

U.S. Geological Survey
Cold Regions Hydrology Project Office
101 12th Avenue, Box 11
Fairbanks, Alaska 99701

CONTENTS

	Page
Symbols and abbreviations	iv
Abstract	1
Introduction	1
Trisection method of geodetic surveying	3
Glacier surface altitude	7
Snow depths	12
Terminus position	13
Glacier motion	14
Ice thickness	14
References	18

FIGURES

Figure 1.--Map showing Knik Glacier, Alaska, location of data sites, and survey monuments	2
2.--Diagram showing schematic comparison of surveying techniques	5
3.--Diagram showing plan view geometry of glacier surface altitude calculation	9
4.--Graph showing geometry of the 2-kilometer transverse profile of the west-facing terminus of Knik Glacier where changes in the terminus are measured	15
5.--Schematic diagram of radar path in glacier	17

TABLES

Table 1.--Knik Glacier surface altitude data	19
2.--Knik Glacier snow measurements	21
3.--Knik Glacier south and north terminus position data	22
4.--Coordinates of index locations along the west-facing terminus of Knik Glacier	24
5.--Position of Knik Glacier terminus near 10 index locations along the west-facing terminus	25
6.--Surveyed positions of Knik Glacier motion markers and horizontal displacement vectors	26
7.--Ice radar depth soundings of Knik Glacier in 1980	26

SYMBOLS AND ABBREVIATIONS

[Number in parenthesis refers to the page where the symbol first appears or where additional clarification may be obtained.]

Symbol	Units (where applicable)	Description
A	--	Monument used for backsight reference; also used as a subscript (4).
AiC	grads	Horizontal angle (5).
Ait	grads	Horizontal angle (4).
B	--	Monument used for backsight reference; also used as a subscript (5).
BiA	grads	Horizontal angle (5).
C	--	Monument used for backsight reference; also used as a subscript (4.)
°C	degrees Celsius	Temperature (16).
Cti	grads	Horizontal angle (4).
Dh	m	Horizontal distance at sea level (4).
Dt	m	Slope distance (5).
I	--	Subscript denoting a fixed "index" horizontal location (8).
MHz	10^6 cycles/second	Frequency, megahertz (16).
NT	--	North Terminus measurements sites (13).
R	m	Horizontal distance in the equation of surface slope (11).
S	m	Separation between ice radar transmitter and receiver antennas (16).
ST	--	South Terminus measurement sites (13).
V	grads	Vertical angle positive up from horizontal (5).
Vxy	m/a	Glacier speed, horizontal component (26).
a	--	Year (26).
a	unitless	Direction number of a line (10).
a	--	Subscript denoting "atmosphere" (16).

Symbol	Units (where applicable)	Description
b	unitless	Direction number of a line (10).
c	unitless	Direction number of a line (10).
c	m/μs	Speed of electromagnetic wave in vacuum (16).
d	--	Subscript denoting "delay" time (16).
f	m^{-1}	Earth curvature and atmospheric refraction coefficient; subscript denotes "curvature and refraction" (7).
g	--	Subscript denoting "glacier" surface (13).
h	m	Ice depth perpendicular to bed (16).
i	--	Survey instrument location, also used a subscript (4).
i	--	Subscript denoting glacier "ice" (16).
j	unitless	Proportionality constant in the equation of a line (8).
k	unitless	A constant (10).
km	--	Kilometer (19).
m	--	Meter (12).
t	μs	Time, in microseconds (16).
t	--	Survey target; also used as a subscript (4).
x	m	Local easterly coordinate at sea level scale (4).
y	m	Local northerly coordinate at sea level scale (4).
z	m	Altitude above sea level (6).
z_g^i	m	Apparent altitude of the glacier surface from ice horizon observation (13).
α	grads	Interior angle at i, trisection survey (4).
β	grads	Interior angle at C, trisection survey (4).
γ	grads	Interior angle at t, trisection survey (4).
Δz	m	Altitude difference (6).

Symbol	Units (where applicable)	Description
$\Delta_{\bar{z}_f}$	m	Vertical error due to earth curvature and atmospheric refraction (6).
ζ	m or km	Curvilinear coordinate transverse to glacier centerline, right-handed system (15).
θ	grads	Polar coordinate horizontal azimuth, positive counterclockwise from east (4).
μs	10^{-6} s	Microseconds (16).
ξ	m or km	Longitudinal curvilinear coordinate at glacier centerline (2).
ϕ	grads	Dip angle at glacier surface (8).

GEODETIC TRISECTION, ALTITUDE, AND ICE-RADAR SURVEYING TECHNIQUES USED AT KNIK GLACIER, ALASKA, AND SUMMARY OF 1979, 1980, AND 1981 DATA

By L. R. Mayo and D. C. Trabant

ABSTRACT

Knik Glacier in south-central Alaska has the potential to re-form Lake George, Alaska's largest glacier-dammed lake. Measurements of surface altitude, snow depth, terminus position, glacier speed, and ice depth are being made in an attempt to determine the mechanisms that could cause a significant readvance of the glacier.

New surveying and data reduction techniques were developed by the authors and employed successfully at Knik Glacier. These include precise geodetic surveying by the "trisection" technique, calculation of surface altitude at a spacially-fixed "index point" from three point measurements on a rough, moving glacier surface, and calculation of ice thickness from low frequency radar measurements. In addition, this report summarizes the data collected from 1979 to 1981 in support of this goal.

INTRODUCTION

Knik Glacier, located in the Chugach Mountains of south-central Alaska, presently calves into the Knik River along a gorge whose west bank is the east-facing flank of Mount Palmer. A minor advance of the glacier would cause Lake George, Alaska's largest recently active glacier-dammed lake (Post and Mayo, 1971), to re-form and thus significantly increase the immediate flood hazard along the Knik River.

Measurements on the glacier in May or June from 1979 to 1981 at sites shown on figure 1 contribute to the data base necessary to determine the possible mechanisms that could re-form Lake George. The 1979 field work established precise geodetic

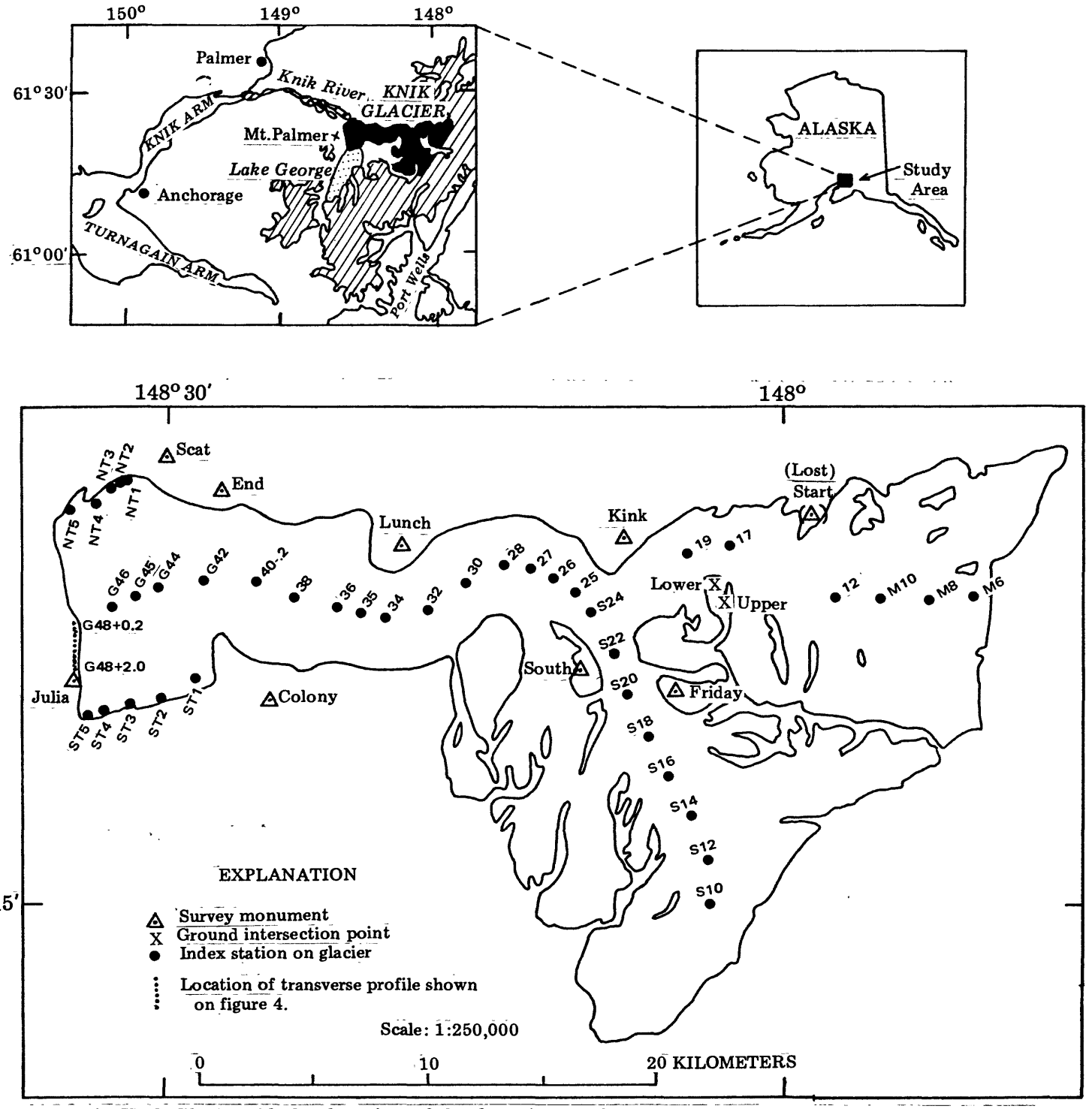

Figure 1.--Knik Glacier, Alaska, location of the data sites, and survey monuments. Stations on the glacier are kilometers from the head of the glacier along the ξ longitudinal coordinate system described by Trabant and Mayo (1979).

coordinate systems for use at Knik Glacier and baseline data on the glacier altitude (Trabant and Mayo, 1979). The 1980 and 1981 measurements were made to determine surface altitude and gradient changes, ice velocity, snow depth, and glacier thickness. The Knik Glacier data are presented in considerable detail in this report because they were obtained and manipulated in a manner that has not been published elsewhere.

This report also describes surveying techniques developed by the authors: a "trisection" method of geodetic surveying utilizes two theodolites, only one of which is at a known location and directly measures the variable earth curvature and atmospheric refraction correction coefficient; and a method of calculating a representative glacier surface altitude at a fixed "index point" on a moving, sloping, rough ice surface. The thickness of glacier ice was determined by a surveying technique that uses low frequency radar. The objective of these new methods is to reduce the time required to accomplish field work and, at the same time, increase the accuracy of surveys when considerable distances are involved.

TRISECTION METHOD OF GEODETIC SURVEYING

Simple surveying techniques cannot be applied at Knik Glacier because of the size of the area and the large expenditure of effort that would be involved. The geodetic surveys of glacier surface altitudes, position of motion markers, and location of ice radar antennas made at Knik included corrections for the effects of earth curvature, variable atmospheric refraction, and scale change with altitude. The techniques used at Knik include the resection, foresight, and intersection (incorrectly termed "triangulation" by Mayo and others, 1979). More recently, another technique was devised termed the "trisection" that was successfully applied at Knik Glacier. The National Mapping Division of the U.S. Geological Survey has occasionally used a similar technique (J. D. McLaurin, 1982, written communication), but to the authors' knowledge the method has not been published. Trisection directly and quickly determines, without the need of a distance measurement, the variable earth curvature - atmospheric refraction correction, and the position and

altitude of a theodolite located at a target. The trisection method is more accurate than any of the other techniques, because all distances are derived from the survey net coordinates, which are more accurate than distances measured along single, unchecked lines. Furthermore, it is the only surveying technique that measures directly the vertical atmospheric refraction along a single observation line. The trisection survey combines geometric elements of the foresight, intersection, and resection techniques.

For the general case, (fig. 2) i and C need not be intervisible; the solution to the trisection survey is as follows:

$$\theta_t = \theta_A - Ait \tag{1}$$

and $$\alpha = \theta_C - \theta_t. \tag{2}$$

Thus, $$\alpha = \theta_C - \theta_A + Ait, \tag{3}$$

$$\gamma = 400 - Cti \quad (\text{Note: } 400^{\text{grads}} = 360°), \tag{4}$$

and $$\beta = 200 - \alpha - \gamma. \tag{5}$$

By combining equations 3, 4, and 5:

$$\beta = \theta_A - \theta_C + Cti - Ait - 200. \tag{6}$$

Using the Pythagorean theorem,

$$Dh_C = \sqrt{(x_C - x_i)^2 + (y_C - y_i)^2} \tag{7}$$

where x and y are the coordinates of known points i and C.

Applying the law of sines to find the horizontal sea level distance, Dh_t, between the known instrument location, (i), and the target instrument, (t),

$$\frac{Dh_t}{\sin\beta} = \frac{Dh_C}{\sin\gamma} \tag{8}$$

or

$$Dh_t = \frac{Dh_C \sin\beta}{\sin\gamma}. \tag{9}$$

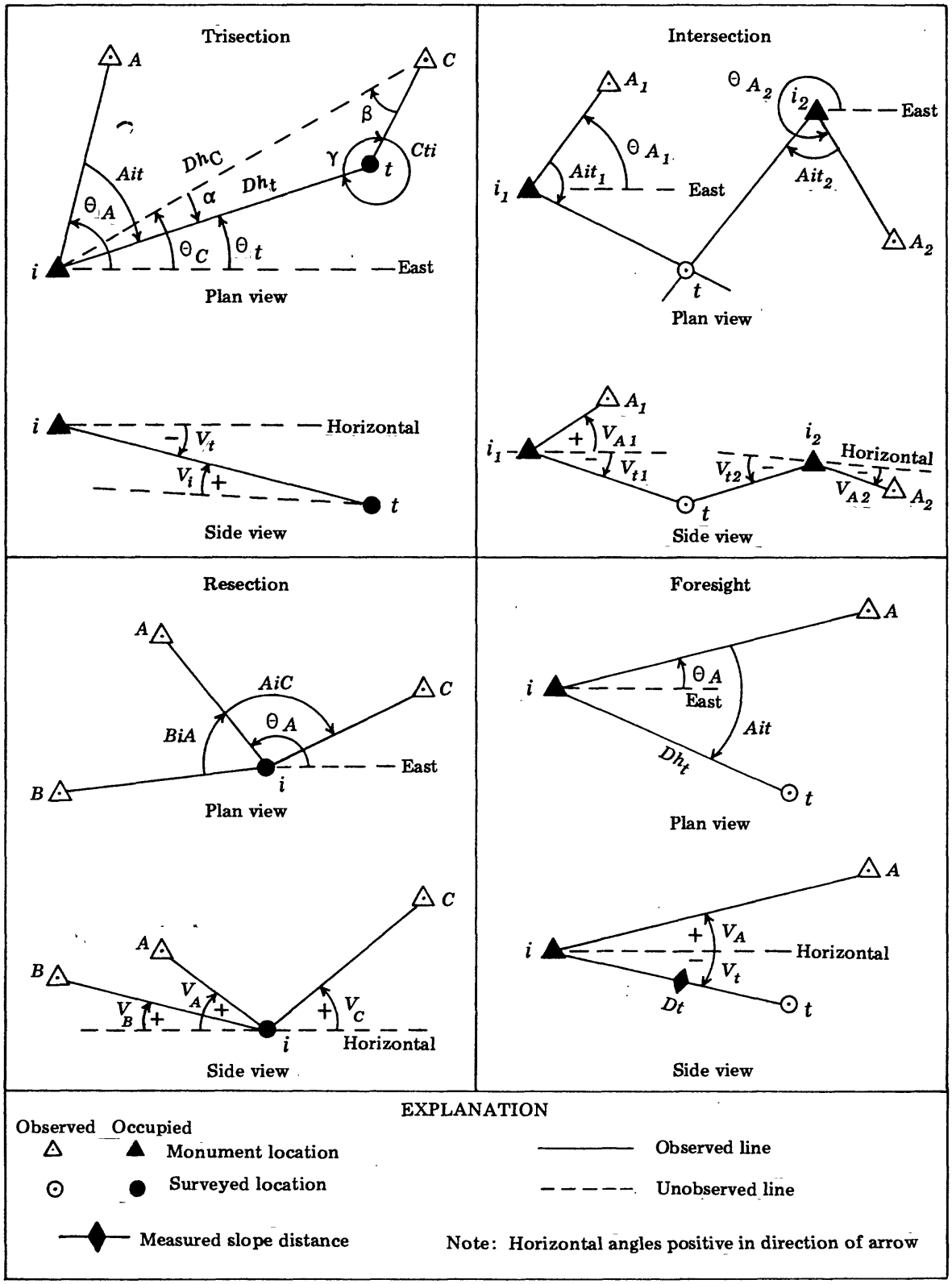

Figure 2.--Schematic comparison of surveying techniques.

By substitution using equations 4, 6, 7, and 9,

$$Dh_t = \frac{\sqrt{(x_C - x_i)^2 + (y_C - y_i)^2} \cdot \sin(\Theta_A - \Theta_C) + Cti - Ait - 200}{\sin(400 - Cti)} \qquad (10)$$

The azimuths Θ_A and Θ_C in equation 10 can be calculated from the survey net coordinates:

$$\Theta_A = \tan^{-1}\left(\frac{y_A - y_i}{x_A - x_i}\right) \qquad (11)$$

and

$$\Theta_C = \tan^{-1}\left(\frac{y_C - y_i}{x_C - x_i}\right) . \qquad (12)$$

Thus the distance, Dh_t, to the target can be calculated using equations 10, 11, and 12 in terms of the survey net coordinates (x_A, y_A), (x_i, y_i), and (x_C, y_C); and the readily measured horizontal angles, Ait and Cti. In this technique a theodolite at the target effectively replaces an electronic distance measuring system used in a foresight survey. From this point on, the geodetic horizontal location of the target instrument is calculated using the foresight equations found in Mayo and others (1979).

The altitude of the trisection target instrument, z_t, can be measured quickly with a degree of confidence usually reserved only for detailed, precise geodetic surveys, where simultaneous vertical angles between theodolites are observed and used to solve the earth curvature - atmospheric refraction problem directly. The difference in altitude, Δz, from the primary instrument, i, to the target instrument, t (the foresight direction), is the average of the foresight and the backsight observations (Moffitt and Bouchard, 1975, p. 80). The plane geometry solutions for Δz are different because of the combined effect that earth's curvature and atmospheric refraction have on the observed horizontal angles (note the nonparallel vertical reference lines in figure 2). In this method, the sign of the backsight angle must be changed.

$$\Delta z = \frac{Dh_t \tan V_t + Dh_t \tan(-V_i)}{2} . \qquad (13)$$

Half of the difference between $Dh_t \tan V_t$ and $Dh_t \tan(-V_i)$ is the vertical error due to curvature and refraction, Δz_f: Thus,

$$\Delta z_f = \frac{Dh_t \tan V_t + Dh_t \tan V_i}{2} . \qquad (14)$$

The curvature-refraction coefficient, f, (see Mayo and others, 1979) can be calculated from the above information. The "error", Δz_f, is expressed as a "correction" by changing sign and can be converted into a more generally useful form where:

$$-\Delta z_f = f\,Dh_t^2 \quad . \tag{15}$$

Combining equations 14 and 15 and solving for the coefficient, f:

$$f\,Dh_t^2 = -\frac{Dh_t\,(\tan V_t + \tan V_i)}{2} \tag{16}$$

or

$$f = -\frac{\tan V_t + \tan V_i}{2\,Dh_t} \quad . \tag{17}$$

The distinct advantage of this surveying practice is that the combined curvature and refraction correction is measured directly with easily obtainable vertical angle data. Knowledge of the coefficient, f, is useful for application to other surveys conducted under similar conditions. Another equally useful approach is to calculate the angular error per standard unit of horizontal distance as is practiced by the National Mapping Division of the U.S. Geological Survey (J. D. McLaurin, 1982, written communication). Both methods assume that curvature and refraction are uniform along the observed line.

The altitude of the trisection target instrument, once the curvature and refraction coefficient, f, has been determined, is calculated by the geodetic foresight solution explained in Mayo and others (1979, p. 4).

GLACIER SURFACE ALTITUDE

The purpose of repeated, precise glacier surface altitude surveys (table 1) is to determine the rate of thickening or thinning at a spacially-fixed "index" location. In practice, precise reoccupation of a location on a glacier is not only time consuming, it may be impossible due to crevasses. Additionally, a more representative altitude on a rough glacier surface can be found by measuring several points rather than by measuring only one. The technique described here enables precise glacier surveys in a minimum of field time. A routine was developed which uses

three surveyed points, $x_1 y_1 z_1$, $x_2 y_2 z_2$, and $x_3 y_3 z_3$ near the index point, $x_I y_I$, to calculate the down-dip surface azimuth, θ, a standard polar coordinate component in the horizontal plane with east as zero and positive in the counterclockwise direction; the dip, ϕ, a vertical angle with horizontal as zero and positive up; and the altitude of the index location, z_I. We assume that the local glacier surface is represented by the plane defined by the three surveyed points (fig. 3).

Even though the mathematical solution to this problem may appear to be a "war of lines", it is more readily programmed and executed than the more common solution using equations of planes and a matrix inversion. A program is available from the authors.

The solution begins with the two-point form of the parametric equations of a line in three dimensions:

$$x_0 = x_1 + (x_2 - x_1) j \tag{18}$$

$$y_0 = y_1 + (y_2 - y_1) j \tag{19}$$

and

$$z_0 = z_1 + (z_2 - z_1) j \tag{20}$$

where $x_0 y_0 z_0$ are the coordinates of all points along a line, and j is a unique proportionality constant for each point along a line defined by the coordinates, $x_1 y_1 z_1$ and $x_2 y_2 z_2$, which may be two surveyed locations. To find the point at which this line reaches the altitude of a third surveyed location, $x_3 y_3 z_3$, let $z_0 = z_3$ in equation 20 and solve for j:

$$j = \frac{z_3 - z_1}{z_2 - z_1} . \tag{21}$$

Substituting this value of j back into equations 18 and 19, we find a point, $x_0 y_0 z_0$, which is the intersection of an altitude contour line through $x_3 y_3 z_3$, and the line defined by $x_1 y_1 z_1$ and $x_2 y_2 z_2$, because $z_0 = z_3$.

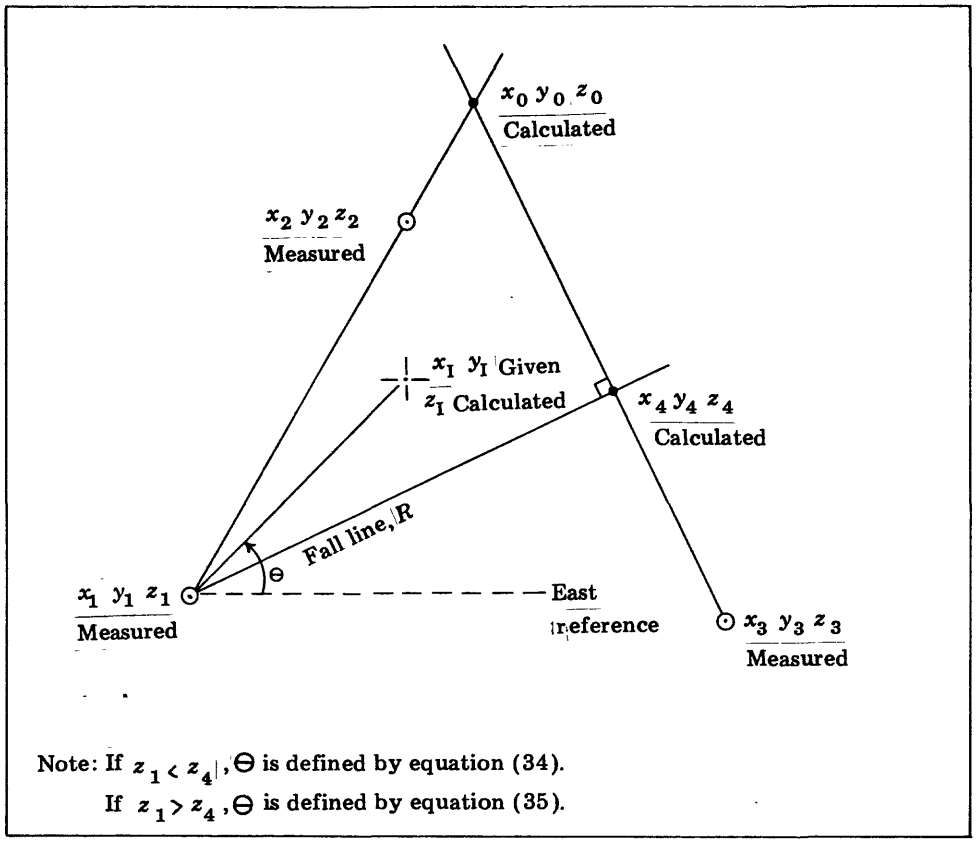

Note: If $z_1 < z_4$, Θ is defined by equation (34).
If $z_1 > z_4$, Θ is defined by equation (35).

Figure 3.--Plan view geometry of glacier surface altitude calculation.

The parametric equations for the contour line are thus:

$$x = x_3 + (x_0 - x_3)j \tag{22}$$
$$y = y_3 + (y_0 - y_3)j \tag{23}$$
$$z = z_3 \tag{24}$$

where j is defined by equation 21.

Eliminating j and solving for y,

$$y = y_3 + (y_0 - y_3)\left(\frac{x - x_3}{x_0 - x_3}\right). \tag{25}$$

In equations 22 and 23, $x_0 - x_3$ and $y_0 - y_3$ are direction numbers. From solid geometry two lines are perpendicular if and only if their direction numbers are such that: $a_1 a_2 + b_1 b_2 + c_1 c_2 = 0$.
In this case c_1 and c_2 are zero and by making $a_2 = -b_1$ and $b_2 = a_1$ we have direction numbers for a line perpendicular to the contour line.

Using these direction numbers, the equations for the line perpendicular to the contour line, a fall line, may be written as,

$$x = x_3 + (y_3 - y_0)j \tag{26}$$
$$y = y_3 + (x_0 - x_3)j. \tag{27}$$

Eliminating j and solving for y,

$$y = k + y_3 + (x_0 - x_3)\left(\frac{x - x_3}{y_3 - y_0}\right), \tag{28}$$

where k is a constant evaluated at a known point, $x_1 y_1 z_1$, so that equation 28 is the fall line through one of the surveyed locations. Therefore,

$$k = y_1 - y_3 - (x_0 - x_3)\left(\frac{x_1 - x_3}{y_3 - y_0}\right). \tag{29}$$

Point $x_4 y_4 z_4$, the intersection of the contour line (equation 25) and the fall line through the first surveyed location (equation 28), is now found by equating the two expressions, solving for x, and letting $x = x_4$:

$$x_4 = x_3 + \left[\frac{k}{\left(\frac{y_0 - y_3}{x_0 - x_3}\right) - \left(\frac{x_0 - x_3}{y_3 - y_0}\right)} \right] ; \qquad (30)$$

the value y_4 may be found by substitution of x_4 for x into either equations (25) or (28); and $z_4 = z_0 = z_3$.

The horizontal distance R between $x_1 y_1 z_1$ and $x_4 y_4 z_4$ is given by

$$R = \sqrt{(x_1 - x_4)^2 + (y_1 - y_4)^2} \; . \qquad (31)$$

The vertical difference, Δz, is

$$\Delta z = z_1 - z_4 \; . \qquad (32)$$

The vertical angle of the fall line or dip of the plane, ϕ, is:

$$\phi = \tan^{-1}\left(\frac{\Delta z}{R}\right) \qquad (33)$$

and the azimuth of the down-dip direction is:

$$\theta = \tan^{-1}\left(\frac{y_1 - y_4}{x_1 - x_4}\right) \quad \text{if } z_4 > z_1 \qquad (34)$$

or $$\theta = \tan^{-1}\left(\frac{y_4 - y_1}{x_4 - x_1}\right) \quad \text{if } z_4 < z_1 \; . \qquad (35)$$

The altitude of the fixed index location, $x_I y_I$, or any other specified location can be calculated from the coordinates of one of the surveyed locations, $x_1 y_1 z_1$, and the dip, ϕ, and dip-azimuth, Θ, of the surface-representing plane by:

$$z_I = z_1 + R(\tan\phi)\cos(\Theta_I - \Theta) \tag{36}$$

where $$R = \sqrt{(x_I - x_1)^2 + (y_I - y_1)^2} \tag{37}$$

and $$\Theta_I = \tan^{-1}\left(\frac{y_I - y_1}{x_I - x_1}\right). \tag{38}$$

The accuracy of each survey at Knik Glacier was limited primarily by variable atmospheric refraction in the vertical and by the rough glacier surface. Small errors in horizontal position, estimated to be less than ±0.30 m, do not contribute significantly to altitude uncertainty because the vertical angle of most surveys was less than 10^g. At Knik Glacier f was usually determined within $\pm 5 \times 10^{-9}$ m^{-1} which is an altitude accuracy of about ±0.10 m. Roughness of the ice surface in some locations causes a problem in defining the height of the "average ice surface". Generally, determination of the average surface was within ±0.05 m. Where the ice is very rough the surface definition was estimated (table 1).

SNOW DEPTHS

Measurements of snow depth are possible at Knik using probe rods where the snow overlies solid ice. In the accumulation zone the only measurement to date was made by observing the snow stratigraphy on a crevasse wall. To the authors' knowledge, that measurement of 17 m of snow (table 2) represents the thickest measured snowpack ever observed on the North American Continent. Reliable and quick techniques for measuring such deep snow packs in the accumulation zones of glaciers are not available at this time, but research to develop such techniques is presently under way.

TERMINUS POSITION

The terminus of Knik Glacier is measured each year at 20 locations: 5 along the south-facing terminus (ST on fig. 1), 10 along the west-facing ice gorge where the glacier calves into the Knik River (ξ = G48 on fig. 1), and 5 along the north-facing terminus (NT on fig. 1). The curvilinear coordinate, ξ , in this report is equivalent to the x' coordinate in Trabant and Mayo (1979).

The south terminus is surveyed from station COLONY. Each year, the theodolite is set to the same vertical angle for each point to be surveyed, then the horizontal angle is varied until the cross hairs intersect the terminus as interpreted through the telescope. Parts of the south terminus are covered by thick supraglacial moraine, so the interpretation is not precise. The position can be calculated by the foresight technique; but more simply, the change in position, $\Delta \xi$, (table 3) can be approximated from the observed change of grid azimuth, $\Delta \Theta_t$, of the line-of-sight to the ice front using the following simple relationship:

$$\Delta \xi = Dt \cos V_t \sin (\Delta \Theta_t) \qquad (39)$$

where Dt is the slope distance between the theodolite and the target and V_t is the vertical angle, as previously defined for other surveys in this paper.

The north terminus is surveyed by the same technique but from survey station SCAT. The north terminus is not hidden under as much morainal debris as the south terminus, so the north terminus surveys are more accurate. In this case, however, $\Delta \xi$ is positive in the negative $\Delta \Theta_t$ direction, so :

$$\Delta \xi = -Dt \cos V_t \sin (\Delta \Theta_t) \ . \qquad (40)$$

The terminus at the 10 west-facing ice gorge sites is very difficult to survey. We survey either the top of the ice cliff using intersection techniques and a hovering helicopter as the target (z_g in table 5), or we survey only the height of the ice horizon at the terminus as it is viewed from survey station COLONY (z'_g in table 5). These two types of vertical surveys do not give identical results because the

top of the ice cliff is not always visible from COLONY. Intersection on a hovering helicopter is not always possible due to high winds. In 1981, both types of surveys were performed simultaneously to provide a comparison.

The ice-gorge terminus is measured along sight lines radiating from station COLONY to index locations G48 + 0.2 to G48 + 2.0. (See figure 4.) Coordinates of the index locations (table 4) are simply subdivisions of the lines between the index location coordinates defined earlier (Trabant and Mayo, 1979, p. 14).

Due to the random, local changes along a calving ice face, the average terminus position, $\bar{\xi}$, best expresses the sense and magnitude of the gross change in position. Changes in position, $\Delta\xi$, (table 5) of the west-facing terminus cause changes predominantly in the x coordinate of the surveyed points. Therefore, the average terminus position along the longitudinal coordinate, $\bar{\xi}$, was approximated as a function of the average x coordinates of the surveyed points.

$$\bar{\xi} = \xi_I - (\bar{x}_t - \bar{x}_I) \qquad (41)$$

where $\xi_I = 48{,}000$ m and $\bar{x}_I = 15932.1$ m.

GLACIER MOTION

Motion markers made from lead-weighted fish nets and orange oilcloth were placed at four points on the glacier in 1980. These were recovered, resurveyed, and moved in 1981. The horizontal displacement vectors of the markers are given in table 6. The motion of the glacier is somewhat different from that of the markers however, because a marker rides on the ice surface only, rather than with a particular ice particle in the glacier. Unrecovered markers are listed because they may eventually be found.

ICE THICKNESS

A monopulse glacier radar system (Watts and Wright, 1981) was modified for greater power and used at four sites in May 1980 to obtain basal reflections from Knik

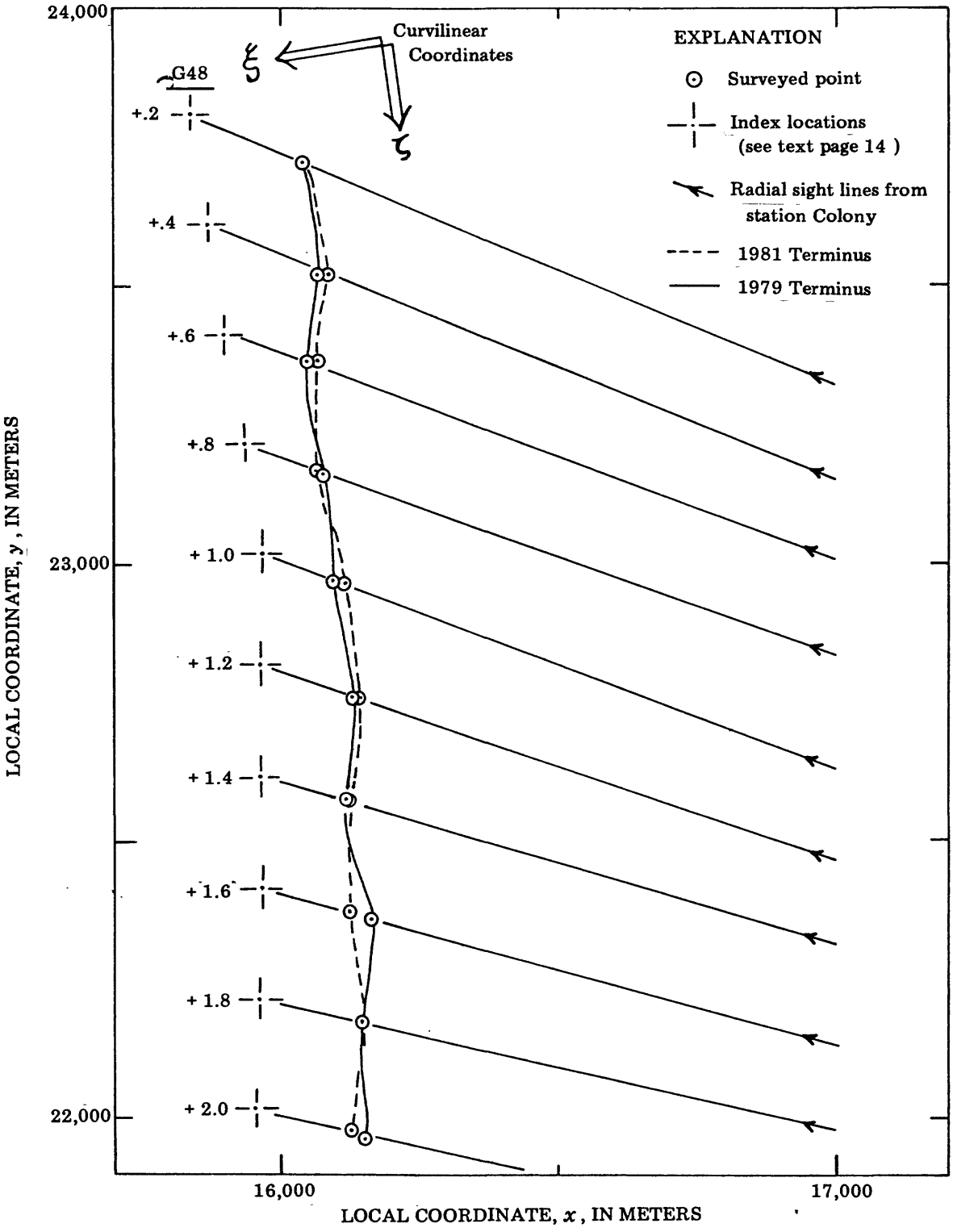

Figure 4.--Geometry of the 2-kilometer transverse profile of the west-facing terminus of Knik Glacier where changes in the terminus are measured.

Glacier (table 7). The transmitter and receiver components are separated by a distance, S, to prevent receiver overloading and antenna ringing. Ice thickness, h, the slope distance from a point between the transmitter and receiver to the nearest area of glacier bed, is determined by measuring the delay time, t_d, in microseconds, between the arrival at the receiver of the airborne wave and the reflected wave.

For figure 5 the Pythagorean theorem states that:

$$\overline{BR}^2 = h^2 + \left(\frac{S}{2}\right)^2 ; \tag{42}$$

and since

$$\overline{BR} = \overline{TBR}/2 , \tag{43}$$

then

$$h = \sqrt{\left(\frac{\overline{TBR}}{2}\right)^2 - \left(\frac{S}{2}\right)^2} \tag{44}$$

or

$$h = \frac{\sqrt{(\overline{TBR})^2 - S^2}}{2} . \tag{45}$$

The path length of the radar signal in ice, $\overline{TBR}$, can be calculated if the time and speed of travel of the radar pulse in both air and ice are known. The radar signal is transmitted simultaneously into the air above the glacier and into the ice. The receiver oscilloscope which measures only delay of time, t_d, is triggered by the arrival of the airborne wave. Therefore, the total travel time in ice, t_i, is the sum of the travel time in air, t_a, plus the time between the arrival of the air wave and reflected wave, t_d, measured at the receiver.

$$t_i = t_d + t_a . \tag{46}$$

The speed of radio waves in air, c_a, is approximately that for a vacuum, c = 299.8 m/μs. The speed in ice, c_i, is determined by the magnetic permittivity of ice at 0°C for the radar frequency, 1.7 MHz.

Jiracek and Bentley (1966, p. 319) measured a speed of 168.5 ± 1.0 m/μs on the Skelton Glacier, a cold, -20°C, glacier in Antarctica using 30 MHz radio waves. Information from three review papers on the electromagnetic properties of ice

(Evans, 1965; Dorsey, 1968; and Robin, 1975) indicate that radio wave velocity has not been measured for waves of 1.7 MHz through 0°C glacier ice. These papers do not indicate with certainty that radio waves propagate significantly more slowly in 0°C ice at 1.7 MHz frequency than in -20°C ice, although future measurements may prove otherwise. Thus for now we assume that a 1.7 MHz radar pulse propagates at a speed, c_i = 168 m/μs, in 0°C glacier ice. This corresponds to a relative permittivity of 3.17 and an index of refraction of 1.78.

Because $$\overline{TBR} = c_i t_i \quad (47)$$

or $$\overline{TBR} = c_i (t_d + t_a), \quad (48)$$

and because $$t_a = S/c_a, \quad (49)$$

$$\overline{TBR} = c_i (t_d + S/c_a). \quad (50)$$

Combining equation 45 with 50 to solve for ice thickness,

$$h = \frac{\sqrt{[c_i (t_d + S/c_a)]^2 - S^2}}{2} \quad (51)$$

or $$h = \frac{\sqrt{[168(t_d + S/299.8)]^2 - S^2}}{2}. \quad (52)$$

Measured ice depths at Knik Glacier are listed in table 7.

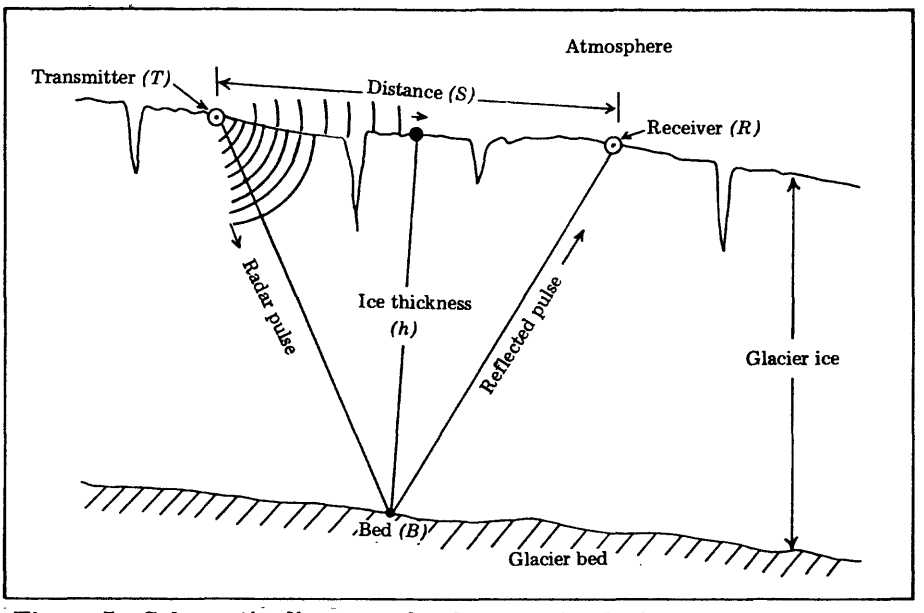

Figure 5.--Schematic diagram of radar path in glacier.

REFERENCES

Dorsey, N. E., 1968, Properties of ordinary water-substance: New York, Hafner Publishing Co., 673 p.

Evans, S., 1965, Dielectric properties of ice and snow - A review: Journal of Glaciology, v. 5, no. 42, p. 773-792.

Jiracek, G. R., and Bentley, C. R., 1966, Dielectric properties of ice at 30 Mc./sec.: Journal of Glaciology, v. 6, no. 44, p. 319.

Mayo, L. R., Trabant, D. C., March, Rod, and Haeberli, Wilfried, 1979, Columbia Glacier stake location, mass balance, glacier surface altitude, and ice radar data, 1978 measurement year: U.S. Geological Survey Open-File Report 79-1168, 72 p.

Moffitt, F.H., and Bouchard, Harry, 1975, Surveying (6th ed.): New York, Harper and Row, 879 p.

Post, Austin, and Mayo, L.R., 1971, Glacier-dammed lakes and outburst floods in Alaska: U.S. Geological Survey Hydrologic Investigations Atlas HA 455, 10 p., 3 pl.

Robin, G. de Q., 1975, Velocity of radio waves in ice by means of a bore-hole interferometric technique: Journal of Glaciology, v. 15, no. 73, p. 151-159.

Trabant, D. C., and Mayo, L. R., 1979, Knik Glacier, Alaska, May 1979 monument and glacier survey: U.S. Geological Survey Open-File Report 80-48, 20 p., 2 pl.

Watts, R. D., and Wright, D. L., 1981, Systems for measuring thickness of temperate and polar ice from the ground or from the air: Journal of Glaciology, v. 27, no. 97, p. 459-469.

Table 1.--Knik Glacier surface altitude data, 1979, 1980, and 1981. Index locations on the glacier are specified by the curvilinear coordinate ξ. (See fig. 1.) The glacier surface altitude, z_I, is calculated from the coordinates of one surveyed point, xyz, near the index point and the surface slope, θ and ϕ. Values in parentheses were measured, but on a different date. Surface slopes measured from maps are designated by an asterisk (*). The angular unit "grad" is 1/100th of a right angle. Where accuracy is not specified it is better than ±0.1 m. Surface slope measurements made in 1980 and applied to the 1979 point measurements (Trabant and Mayo, 1979, p. 20) result in the 1979 index point altitudes reported here.

Site ξ (km)	Date (YY.MMDD)	Glacier surface survey Local coordinates x (m)	y (m)	z (m)	Surface slope Direction θ (grads)	Dip ϕ (grads)	Index point Altitude z_I (m)	Accuracy ± (m)
M10	79.0524	50904.5	24238.0	2267.6	199.58	-3.67	2265.1	0.1
19	79.0524	42401.0	26343.5	1454.6	(266.86)	(-3.67)	1454.4	0.1
25	79.0524	37358.5	24569.3	863.8	(100.32)	(-6.64)	864.1	0.1
30	79.0523	32683.0	25245.2	709.3	(301.66)	(-2.36)	709.3	0.1
35	79.0523	28252.0	23880.7	527.6	(160.04)	(-7.13)	527.5	0.5
40	79.0523	23473.5	25389.8	375.0		(moraine)		
G45	79.0523	18601.1	25075.9	241.6	(unmeasured)		239.5	0.5
S12	79.0524	43013.6	12939.2	1619.2	160	-2.16*	1618.8	0.2
S18	79.0524	40644.7	18448.5	1367.2	(185.06)	(-7.53)	1366.8	0.1
M10	80.0603	50854.0	24308.4	2268.8	(199.58)	(-3.67)	2269.2	0.1
19	80.0509	42382.3	26340.5	1454.9	266.86	-3.67	1455.3	0.1
25	80.0507	37361.9	24572.2	863.8	100.32	-6.64	864.4	0.1
30	80.0507	32682.0	25246.3	709.2	301.66	-2.36	708.2	0.1
35	80.0507	28209.6	23800.6	524.8	160.04	-7.13	523.3	0.5
40-0.2	Newly defined location, ξ =-0.2km x_I 23536.2 y_I 25578.9							
	80.0507	23547.1	25581.3	360.7	167.70	-1.26	360.6	0.1
G45	80.0603	18713.8	25006.4	238.0	(unmeasured)			
S12	80.0509	42947.2	13043.1	1621.3	160	-2.16*	1624.8	0.2
S18	80.0509	40647.1	18446.8	1367.9	185.06	-7.53	1367.2	0.1
M6	81.0610	54843.7	24147.19	2523.0	198	-4.72*	2523.9	
M8	81.0610	52848.0	24146.4	2380.1	198	-4.50*	2380.6	
M10	81.0610	50858.4	24301.9	2268.5	(199.58)	(-3.67)	2268.7	
12	81.0610	48882.6	24613.1	2177.0	198	-11.98*	2177.4	

Table 1.--Continued

Site	Date	Glacier surface survey			Surface slope		Index point	Accuracy
		Local coordinates			Direction	Dip	Altitude	
ξ (km)	(YY.MMDD)	x (m)	y (m)	z (m)	θ (grads)	ϕ (grads)	z_I (m)	$\pm$ (m)
17	81.0610	44330.9	26575.4	1649.6	163	-5.53*	1650.0	
24	81.0611	37403.4	24566.6	865.2	(100.32)	(-6.64*)	863.9	
25	81.0610	37354.9	24566.8	863.9	(100.32)	(-6.64)	863.9	
26	81.0610	36501.4	25089.8	838.8	---	---	838.8	
27	81.0610	35575.3	25471.9	821.8	-191	-2.80*	821.9	
28	81.0610	34626.3	25701.8	749.4	194	-3.44*	748.2	
30	81.0611	32686.0	25243.0	708.2	(301.66)	(-2.36)	708.3	
32	81.0611	31065.9	24068.6	631.3	---	---	631.3	0.5
34	81.0611	29177.0	23535.8	567.5	---	---		0.5
35	81.0611	28208.7	23832.1	520.9	(160.04)	(-7.13)	521.6	0.5
36	81.0611	27274.5	24154.6	480.1	---	---	480.1	0.5
38	81.0611	25398.3	24845.4	432.5	---	---	432.5	
40-0.2	81.0611	23536.5	25578.8	356.4	(167.70)	(-1.26)	356.4	0.2
G42	81.0611	21522.9	25697.7	345.3	---	---	345.3	1.0
G44	81.0611	19551.7	25365.0	241.9	-86	-1.72*	242.5	1.0
G45	81.0612	18622.2	25066.1	235.1	-192	-3.01*	234.1	0.1
G46	81.0612	17657.4	24785.9	166.3	-148	-3.10*	165.4	
S10	81.0610	43081.8	10982.2	1724.8	100	-3.52*	1726.0	
S12	81.0610	43004.3	12963.3	1624.0	160	-2.16*	1624.3	
S14	81.0610	42386.9	14861.1	1558.8	150	-2.16*	1559.2	
S16	81.0610	41551.1	16670.6	1457.9	145	-2.77*	1458.0	
S18	81.0610	40642.7	18451.6	1370.1	(185.06)	(-7.53)	1370.1	
S20	81.0610	39739.8	20234.1	1259.2	155	-5.38*	1258.4	
S22	81.0610	38938.7	22083.1	1058.2	120	-4.84*	1058.9	
S24	81.0610	38062.9	23860.4	925.2	---	---	925.2	

Table 2.--Knik Glacier snow measurements. Estimated accuracy, ±0.10 m. Only the highest station with no snow is listed.

Site ξ (km)	Date (YY.MMDD)	Snow depth (m)
19	79.0524	2.5
25	79.0524	1.4
30	79.0523	0.5
40	79.0523	0.0
19	80.0509	1.9
25	80.0507	3.0
30	80.0507	2.1
35	80.0507	0.8
40-0.2	80.0507	0.5
G45	80.0509	0.0
S18	80.0509	4.3
12	81.0610	17.0
14	81.0610	2.1
17	81.0610	1.8
25	81.0610	1.6
26	81.0610	0.0
S14	81.0610	5.1
S16	81.0610	5.5
S18	81.0610	4.4
S20	81.0610	3.2
S22	81.0610	1.0
S24	81.0610	0.7

Table 3.--Knik Glacier south and north terminus position data, 1979, 1980, and 1981. Constants are underlined; assumed values are in parentheses. Retreat is indicated by a negative change in length, $\Delta_i \xi$.

A--South Terminus surveys from theodolite 0.53 m above station COLONY.

Site	Date (YY.MMDD)	Dt (m)	V_t (grads)	t (grads)	$\Delta \xi$ (m)
ST-1	79.0521	(3724.0)	-16.6087	-210.3840	
ST-2	79.0521	(4720.7)	-14.0296	-203.4162	
ST-3	79.0521	(6319.9)	-10.5948	-200.1173	
ST-4	79.0521	(7301.4)	- 9.2442	-198.2258	
ST-5	79.0521	(7990.1)	- 8.2464	-196.1339	
ST-1	80.0603	(3724.0)	-16.6087	-210.4580	-4
ST-2	80.0603	(4720.7)	-14.0296	-203.4227	-1
ST-3	80.0603	(6319.9)	-10.5948	-200.3508	-23
ST-4	80.0603	(7301.4)	- 9.2442	-198.2574	-4
ST-5	80.0603	(7990.1)	- 8.4264	-196.0356	+12
				Average	-4
ST-1	81.0611	(3724.0)	-16.6087	-223.6593	-741
ST-2	81.0611	(4720.7)	-14.0296	-203.6864	-19
ST-3	81.061	(6319.9)	-10.5948	-200.5941	-24
ST-4	81.0611	(7301.4)	- 9.2442	-198.4820	-25
ST-5	81.0611	(7990.1)	- 8.4264	-196.0511	-2
				Average	-162
ST-1	81.0612	3724.0	-16.6087	-220.4400	-565
ST-2	81.0612	4720.7	-14.0296	-203.4121	1
ST-3	81.0612	6319.9	-10.5948	-200.5759	-22
ST-4	81.0612	7301.4	- 9.2442	-198.4541	-22
ST-5	81.0612	7990.1	- 8.4264	-196.1214	-11
				Average	-124

Table 3.--Continued

B--North terminus surveys from theodolite 0.85 m above station SCAT.

Site	Date (YY.MMDD)	Dt (m)	V_t (grads)	t (grads)	$\Delta\xi$ (m)
NT-1	79.0523	2267.1	-10.3756	-164.6369	
NT-2	79.0523	2510.8	- 9.4920	-166.1130	
NT-3	79.0523	3032.2	- 7.9293	-164.9778	
NT-4	79.0523	(3855.2)	- 6.2771	-163.6838	
NT-5	79.0523	(5144.9)	- 5.0007	-167.6807	
NT-1	80.0507	(2267.1)	-10.3756	-163.7622	-31
NT-2	80.0507	(2510.8)	- 9.4920	-164.8691	-49
NT-3	80.0507	(3032.2)	- 7.9293	-163.8592	-53
NT-4	80.0507	3855.2	- 6.2771	-162.7016	-59
NT-5	80.0507	5144.9	- 5.0007	-167.8222	+11
				Average	-36
NT-1	81.0611	(2267.1)	-10.3756	-165.3023	54
NT-2	81.0611	(2510.8)	- 9.4920	-165.0214	6
NT-3	81.0611	(3032.2)	- 7.9293	-164.4274	27
NT-4	81.0611	(3855.2)	- 6.2771	-162.9494	15
NT-5	81.0611	(5144.8)	- 5.0007	-168.0430	18
				Average	24

Table 4.--Coordinates of index locations along the west-facing terminus of Knik Glacier. The azimuths θ are from station COLONY to each index point.

Index location $\xi + \zeta$ (km)	Azimuth θ (grads)	Local coordinates x (m)	y (m)
G48 + 0.2	-225.5785	15838.2	23806.7
G48 + 0.4	-224.3825	15869.5	23609.1
G48 + 0.6	-223.1593	15900.9	23411.5
G48 + 0.8	-221.9088	15932.2	23214.0
G48 + 1.0	-220.6286	15963.4	23016.2
G48 + 1.2	-219.2364	15963.4	22816.1
G48 + 1.4	-217.8257	15963.4	22616.1
G48 + 1.6	-216.3960	15963.4	22416.0
G48 + 1.8	-214.9493	15963.4	22215.9
G48 + 2.0	-213.4866	15963.4	22015.8

Table 5.--Position of Knik Glacier terminus near 10 index locations along the west-facing terminus, z_g, is the altitude at the terminus. z'_g is the altitude of the terminus as viewed from station COLONY.

Site $\xi + \zeta$ (km)	Date (YY.MMDD)	Terminus position x (m)	y (m)	z_g (m)	z'_g (m)	$\Delta\xi$ (m)
G48 + 0.2	79.0523	16045.1	23720.5	103.3	---	
G48 + 0.4	79.0523	16072.2	23520.1	108.3	---	
G48 + 0.6	79.0523	16051.6	23362.1	103.4	---	
G48 + 0.8	79.0523	16078.9	23159.0	100.9	---	
G48 + 1.0	79.0523	16100.4	22969.5	104.1	---	
G48 + 1.4	79.0523	16137.2	22758.3	97.2	---	
G48 + 1.2	79.0523	16123.2	22574.0	102.8	---	
G48 + 1.6	79.0523	16167.9	22360.9	100.3	---	
G48 + 1.8	79.0523	16152.1	22173.3	92.4	---	
G48 + 2.0	79.0523	16159.0	21965.3	107.5	---	
	Average x	16108.8	Average	102.0		
	Average ξ	47823.3				
G48 + 0.2	80.0603	---	---	---	103.5	
G48 + 0.4	80.0603	---	---	---	105.8	
G48 + 0.6	80.0603	---	---	---	101.5	
G48 + 0.8	80.0603	---	---	---	95.6	
G48 + 1.0	80.0603	---	---	---	102.6	
G48 + 1.2	80.0603	---	---	---	109.0	
G48 + 1.4	80.0603	---	---	---	105.1	
G48 + 1.6	80.0603	---	---	---	106.4	
G48 + 1.8	80.0603	---	---	---	101.9	
G48 + 2.0	80.0603	---	---	---	109.3	
				Average	104.1	
G48 + 0.2	81.0612	16040.9	23721.0	98.8	100.6	
G48 + 0.4	81.0612	16084.9	23522.7	100.8	107.7	
G48 + 0.6	81.0612	16066.3	23348.9	97.1	97.6	
G48 + 0.8	81.0612	16069.5	23165.1	86.7	94.4	
G48 + 1.0	81.0612	16119.9	22964.0	97.5	102.5	
G48 + 1.2	81.0612	16145.4	22759.7	98.2	106.0	
G48 + 1.4	81.0612	16125.7	22569.8	99.3	102.0	
G48 + 1.6	81.0612	16128.7	22372.8	86.4	101.0	
G48 + 1.8	81.0612	16153.8	22170.7	87.6	102.0	
G48 + 2.0	81.0612	16130.8	21980.1	85.0	101.3	
	Average x	16106.6	Average	93.7	101.5	
	Average ξ	47825.5				+ 2.2

Table 6.--Surveyed positions of Knik Glacier motion markers and horizontal displacement vector components Vxy, annual speed, and Θ, horizontal azimuth. The vertical component is not defined by these motion markers that simply rode on the melting surface.

Site ξ (km)	Identification	Date (YY.MMDD)	Marker position x (m)	y (m)	z (m)	Horizontal displacement vector Vxy (m/a)	Θ (grads)
25	Oilcloth	80.0507	37361.9	24572.2	863.8		
25	Oilcloth	81.0611	Not found, covered by snow				
25	Net 50-6	81.0611	37403.4	24566.6	865.2		
30	Oilcloth	80.0507	32681.8	25246.5	709.2		
30	Oilcloth	81.0611	32211.7	24847.9	693.5	562.8	-155.2
		moved to	32686.0	25243.0	708.2		
35	Oilcloth	80.0507	28209.6	23800.6	524.8		
35	Oilcloth	81.0611	Not found, severe crevassing				
40-0.2	Oilcloth	80.0507	23655.5	25531.9	363.1		
40-0.2	Oilcloth	81.0611	23335.1	25698.0	356.4	329.5	169.6
		moved to	23536.5	25578.8	356.4		

Table 7.--Ice radar depth soundings of Knik Glacier in 1980. S is the separation distance between transmitter and receiver antennas.

Site $\xi + \zeta$ (km)	Antenna System: Mid-point location x (m)	y (m)	z (m)	Separation S (m)	Delay time t_d (μs)	Glacier thickness h (m)
30	32682	25246	709	70	No return	>700
35	28253	23806	527	100	6.5	570
40-0.2	23665	25561	363	60	6.8	590
G45.1 + 0.3	18697	24626	235	69	4.4	390